




# Experimental Investigation on Temperature Profiles at Ceiling and Door of Subway Carriage Fire

Min Peng, Xudong Cheng \* and Wei Cong, State Key Laboratory of Fire Science, University of Science and Technology of China, Hefei, Anhui 230026, People's Republic of China

Richard Yuen, Department of Civil and Architectural Engineering, City University of Hong Kong, Hong Kong 999077, People's Republic of China

**Received:** 21 December 2019/**Accepted:** 13 June 2020

**Abstract.** Previous studies usually used the common tunnel model and paid little attention to the propagation characteristics of fire in the carriage structure with multiple lateral openings. In the current study, experiments were carried out in a reduced-scale (1:5) subway carriage model to study the propagation characteristics of carriage fire. The main focuses were on the temperature contour profiles and distribution laws under the ceiling and at different doors inside the carriage. Results show that although the status of the side door of the carriage does not have a significant effect on the mass loss rate of fuel combustion, the temperature distribution under the ceiling will be affected under the effect of the smoke overflow of the door opening. The effect of door status on the longitudinal ceiling temperature is mainly on the area between the fire source and the adjacent door. For the transverse ceiling temperature above the fire source, the effect of the status of the door is significant with the increase of the fire source. Besides, the temperature contour profile at the door shows regular distribution. In the process of gradually increasing the temperature as the height increases, the isotherm gradually changes from a horizontal straight line to two inverted triangular sides, the temperature at the door has been basically in the ambient temperature from the dimensionless height (normalized by the height of the door) below 0.6. The measured radiation at the upper part of the carriage end is about 5 times higher than that in the middle of the door adjacent to the fire source, and the ratio is not significantly affected by the heat release rate. The results of this study can be of use to the fire-protection community to better understand fire dynamics.

**Keywords:** Temperature decay profile, Isotherm contour, Door status, Radiant heat flux, Carriage fire, Subway tunnel

## List of Symbols

$H$	Subway carriage height (m)
$H_d$	Door height (m)
$L$	Model size (m)

\* Correspondence should be addressed to: Xudong Cheng, E-mail: [chengxd@ustc.edu.cn](mailto:chengxd@ustc.edu.cn)



$\dot{m}''$	Mass loss rate per unit area ( $\text{g m}^{-2} \text{s}^{-1}$ )
$Q$	Heat release rate (kW)
$t$	Time
$T$	Temperature (K)
$\Delta T$	Temperature rise (K)
$\Delta T_{l-difference}$	The longitudinal temperature differences between different door statuses
$\Delta T_{t-difference}$	The transverse temperature differences between different door statuses
$\Delta T_{lm}$	Maximum temperature rise at the longitudinal centerline (K)
$\Delta T_{tm,x}$	Maximum transverse temperature rise at a distance of $X$ from the fire source (K)
$\Delta T_{max,d}$	Maximum temperature rise at the door (K)
$W$	Subway carriage width (m)
$X$	Longitudinal distance from the fire source (m)
$Y$	Transverse distance from the fire source (m)
$Z$	Height from the bottom of the door (m)

### Subscripts

$F$	Full scale
$M$	Model scale

## 1. Introduction

Nowadays, the wide use of the subway system provides great convenience for fast transportation in the cities. With the number of subway system continues to increase, various accidents occur during the operation of the system, especially the fire accidents which cause severe consequences due to its complex structure and concentrated personnel [1]. In the twenty-first century, there have been some notable subway fire accidents including the Daegu Subway fire in South Korea killed 198 people and injured 147 people (2003), the Moscow subway fire accident killed more than 40 people and injured over 100 people (2004) and the Hong Kong subway arson incident injured 18 people (2017) [2–4], etc. Hence, fires in subway systems considering subway tunnels and carriages have attracted extensive research attention in recent years.

When a fire occurs in such a narrow and confined space, the plume of heat and toxic products rises from the fire and spreads radially outward over the ceiling, posing a great threat to the building structure, facilities and trapped people [5]. In practice, most of the devices associated with detection, protection, and suppression of fire are located near the ceiling surface. The propagation characteristics of carriage fire, especially the characteristic parameters of the ceiling jet flow, such as the ceiling temperature and distribution, largely determine the effectiveness of the ceiling-mounted detection and protection systems, such as the response of sprinklers, heat detectors and smoke detectors under the ceiling [6]. Therefore, it is necessary to quantify the magnitude and distribution of parameters characterizing propagation characteristics, especially the gas temperature under the ceiling and at typical openings.

Previous studies have been carried out from the perspective of ceiling temperature in tunnel fires and standard compartment fires. In terms of tunnel fires, Zhao et al. [2, 7] carried out experiments and numerical simulations to study the smoke

movement and temperature distribution in a metro tunnel. The effects of non-axisymmetric cross section and longitudinal ventilation on the temperature distribution below the ceiling in metro tunnel fires were investigated. Based on the measured ceiling temperature, Zhang et al. [3, 8] investigated the influence of metro train on the smoke back-layering in the subway tunnel fires, a new physical model including the factor of metro train length was developed to predict the length of smoke back-layering in the tunnel. Meng et al. [9] investigated the smoke flow temperature beneath the tunnel ceiling for a train on fire stopping beside a subway station. The correlations for predicting the longitudinal temperature decay of smoke flow beneath the tunnel ceiling were analyzed and developed. However, for the structure of subway carriages, it not only has the narrow and confined structure similar to the tunnel but also has the special feature of multiple lateral openings (carriage doors on the side). The presence of the lateral openings is likely to affect the fire development in the carriage, and then change the temperature distribution characteristics inside the carriage.

Also, considerable research has been performed to investigate the gas temperature for fires in the standard compartment with side opening. The most commonly used assumption pertains to the one-zone model, in which the entire compartment is assumed to be filled with fire gases of uniform temperature [6]. For example, based on the energy balance for adiabatic conditions, Delichatsios et al. [10] presented a new correlation to predict the gas temperature inside the compartment; Tang et al. [11] carried out the fire experiments in a cubic fire compartment with window to study the temperature profile of buoyant window spill plume from an under-ventilated compartment fire. In these experimental scenarios, the temperature profiles inside the compartment were all considered to be spatially uniform. However, in the event of a fire inside the carriage, the length of the carriage is significantly greater than its height and width, the high-temperature smoke generated by the fire is mainly concentrated in the upper part of the carriage, spreads along the carriage and continuously exchanges heat with the cooler wall surface and the surrounding environment, causing a significant reduction in the temperature [12, 13]. Therefore, it can be deduced that the internal behavior of the carriage fire is different from that of a standard compartment fire.

Concerning train/carriage fires, researches covered many important factors in carriage fires that were carried out in model or real carriages. For example, Ingason [14] performed a series of model scale passenger train fire tests to investigate the effect of parameters including the ventilation, fuel load and the type of interior surface material on the fire development; Li et al. [15] carried out the fire development analysis of three series of train carriage fire tests in different scales (1:10, 1:3 and 1:1), and concluded that the mechanism of fire development was very similar in different scales; Lönnermark et al. [16] carried out tests to study the parameters that control the initial fire spread and the development to local flashover in the 1/3 metro carriage; Chow et al. [17] investigated flame color of train car fire under limited ventilation, revealed that the burning characteristics of a fire in a modern passenger train car depended on oxygen supply and fuel surface area for the same fire load. Cheng et al. [18] conducted the experiments in a reduced-scale subway train model to study the longitudinal and transverse temper-

ature distributions beneath the train ceiling by considering different fire locations and door statuses. Although these works involved a qualitative systematic investigation of the fire development, the quantitative research on the parameters characterizing propagation characteristics of carriage fire has rarely been performed.

This literature review indicates that the propagation characteristics, especially the gas temperature, are recognized as important features for detection and protection in building fires. However, there are few quantitative studies on the gas temperature inside the carriage fire, and the discussion of the influence of the lateral openings on the temperature distribution characteristics under the ceiling of carriage fire needs further supplementation. Therefore, in the current study, experiments were conducted to study the temperature profiles inside the carriage. The main focuses were on the temperature contour profiles and distribution laws under the ceiling and at different doors, the effects of the door status on the longitudinal and transverse ceiling temperature were also taken into account. Furthermore, the mass loss rate, radiant heat fluxes at different positions were also discussed.

## 2. Experimental Setup

The high cost of full-scale experiments seriously hampers its practical usages [19]. Therefore, reduced-scale experiments have been widely carried out. To address the connection between the model scale and the real scale experiments, the Froude Scaling Law has been applied to build up the physical scale model [20–23]. By holding the Froude number constant, correlations for the heat release rate,  $Q$ , time,  $t$  and temperature,  $T$  were established between the model and the real scale tunnel, given in Eq. (1).

$$\frac{Q_M}{Q_F} = \left(\frac{L_M}{L_F}\right)^{5/2}, \quad \frac{t_M}{t_F} = \left(\frac{L_M}{L_F}\right)^{1/2}, \quad T_M = T_F \quad (1)$$

where  $L$  denotes the model size, The subscript ‘ $M$ ’ and ‘ $F$ ’ represent the model and real scale parameters respectively.

The real carriage structure was taken into account when the Froude Scaling Law was used to scale the dimensions. The actual ceiling of the carriage is contoured, but the overall curvature of the contour is small. And many previous studies [4, 9, 15, 17] on the carriages have ignored the contour of the ceiling and regarded it as flat. Therefore, the ceiling structure of the model carriage was also set flat in this experimental setup. The model scale carriage in the experiment was 4.0 m long, 0.55 m wide and 0.42 m high with a scale ratio of 1:5, as shown in Fig. 1. Also, four identical doors with dimensions of 0.26 m wide and 0.38 m high are evenly located at one side of the carriage. The side with doors was made of 8 mm thick fire-resistant glass to observe the experimental phenomena, the ceiling, floor and the other side without doors were made of a 25 mm thick fire-resistant board.

Methanol was used as the fuel and loaded into steel pans to simulate carriages with liquid fuels. In fact, pool fires were burned with two representative kinds of

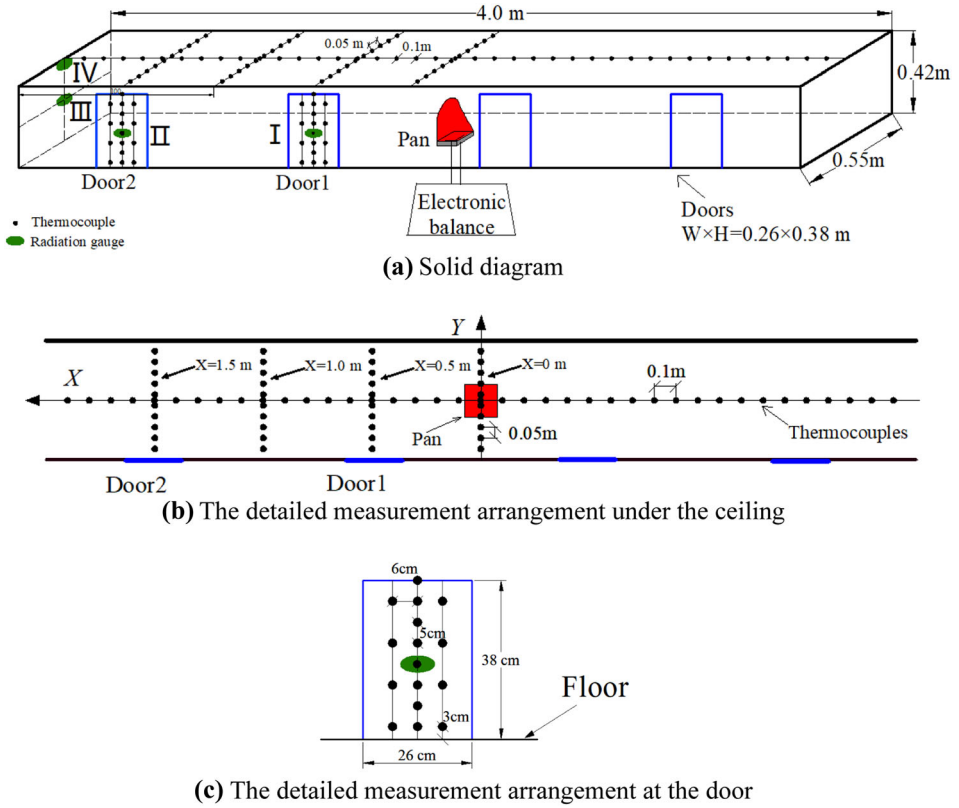


**Figure 1. Schematic of experimental apparatus.**

fuels used. The burning of a liquid fuel produces a translucent blue diffusive flame and consequently emitting a relatively low levels of thermal radiation, such as methanol, propanol, etc. On the other hand, another liquid fuel produces a yellow diffusive flame with high thermal radiation, such as heptane, gasoline, etc. For the fire scenarios in the carriages, there are many kinds of research using methanol as a fire source done before [24–27]. Therefore, in the current work, methanol as a typical liquid fuel is also used as the burning fuel to carry out the research. In the test, there were 8 square pans with side lengths of 9, 11, 13, 15, 17, 20, 23 and 25 cm while all of these pans were made of 2 mm thick steel plates and have the identical height of 2 cm. The fuel initial depth in each experiment was set as 1 cm before ignition. The fuel mass versus time was recorded dynamically by an electronic balance with a maximum load of 34 kg and an accuracy of 0.1 g. The heat release rate can be calculated by the mass loss rate at a steady-stage together with the combustion efficiency and its effective heat of combustion [6].

The temperatures were measured using K-type thermocouples with a diameter of 1 mm and a response time of less than 1 s. 80 thermocouples were mounted 1 cm below the ceiling to measure the ceiling temperature profile, a set of thermo-

couples with 10 cm interval were mounted along the longitudinal centerline of the carriage, four sets of thermocouples with 5 cm interval were mounted 0, 0.5, 1.0, 1.5 m away from the transverse centerline, respectively, as shown in Fig. 1b. Besides, the temperature profile at the door was also considered, so the thermocouples were placed at door 1 and door 2. The detailed thermocouples positions arrangement at the door is shown in Fig. 1c, a sequence of 8 thermocouples were placed at the centerline of the door, spanning from 3 to 38 cm from the floor with an interval of 5 cm, two sequences of 4 thermocouples were also placed at the door with the distance from the centerline 6 cm, spanning from 3 to 33 cm from the floor with an interval of 10 cm. The ambient temperature during the tests was kept within 298–303 K. Four water-cooled radiation gauges were used to measure the radiant heat flux at different positions. The water-cooled radiation gauges I, II, and III were placed in the center of door 1, door 2 facing inward, and the left end of the carriage facing inward, respectively, the gauges IV was placed directly above the gauges III under the ceiling facing inward, as shown in Fig. 1.

Three series of experiments with different setups were a fire in a large lab approximated as an open space (as a control group), in the center of the carriage with open and closed doors. Each case was repeated three times to assure its reliability and repeatability. A summary of the experimental scenarios is presented in Table 1.

### 3. Results and Discussion

#### 3.1. Mass Loss Rate

Figure 2 shows the mass loss rates in typical cases with different pan sizes and door statuses. As shown, for each pan size, the curves of the mass loss rates under different door statuses over time are similar, which means that the effect of the status of the door on the mass loss rate is not significant under the current experimental conditions. This can be explained with the following analysis. Based on the literature data [4, 6, 18], they investigated the ventilation condition of a compartment with more than one opening. According to Fig. 1a, the ventilation factor in

**Table 1**  
**Experimental Scenarios**

Test No	Pan size (cm)	Experimental location
1–3	9	
4–6	11	
7–9	13	
10–12	15	In the open space/Inside carriage with open doors/Inside carriage with closed doors
13–15	17	
16–18	20	
19–21	23	
22–24	25	

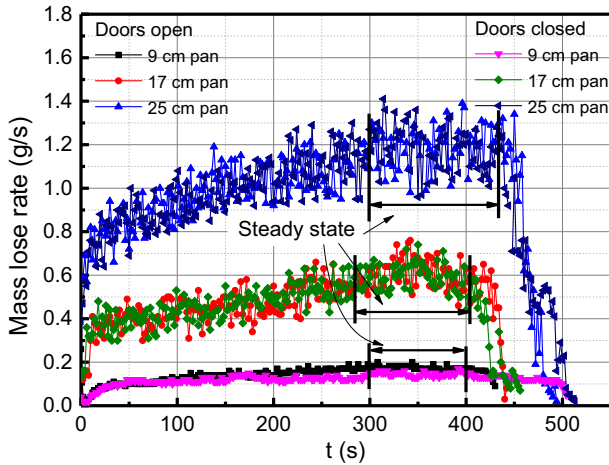


**Figure 2. The mass loss rates in typical cases with different pan sizes and door statuses.**

the case of the door being opened and closed is calculated as 0.543 and 0.299  $m^{5/2}$ , respectively. Then, according to the heat release rate in the compartment defined by Ingason [14], the maximum HRR during the fuel-controlled stage in the case of the door being opened and closed is obtained as 488.7 and 269.1 kW, respectively. These two values are considerably larger than the maximum heat release rate in this experiment (24.5 kW), so all the experimental tests were conducted under well-ventilated conditions. Therefore, the status of the door (open or closed) has insignificant effect on the mass loss rate.

The average mass loss rates per unit area ( $\dot{m}''$ ) at the steady-stage for all tested scenarios are plotted in Fig. 3. It also appears that  $\dot{m}''$  differs very little with the status of the door and remains at around 20  $g/(m^2 s)$ , this value is consistent with the experimental result in Ref.[27]. Besides, the values of  $\dot{m}''$  in the open space are comparable to those inside the carriage, especially in the cases with side length smaller than 17 cm, then determined as a constant at 17  $g/(m^2 s)$ . This result is in agreement with the mass loss rate per unit area and experimentally determined as a constant at 17  $g/(m^2 s)$  when the methanol pool fire with pool diameter higher than 20 cm in Ref.[6].

### 3.2. Temperature Profile

The average longitudinal temperature differences during the steady-state along the ceiling for all fire sizes,  $\Delta T_{l-difference}$ , which are the temperatures under the conditions of open doors minus those under the closed doors, are plotted against the longitudinal distance from the fire source in Fig. 4. It can be observed that the status of the door has a certain effect on the temperature at the longitudinal centerline. Specifically, the temperature difference is always small from door 1 (the nearest door to the fire source) to the end of the carriage, in the range of  $-22.3$

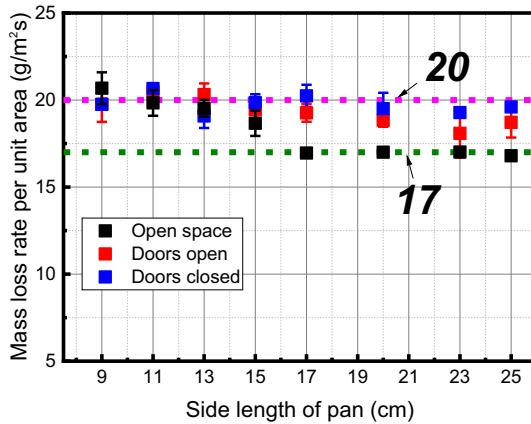


**Figure 3. Mass loss rates per unit area for all tested scenarios.**

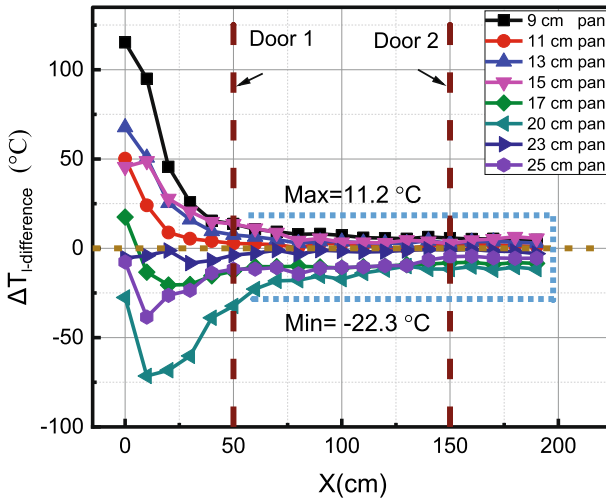


**Figure 4. The longitudinal temperature differences between the statuses of open and closed doors during the steady-state.**

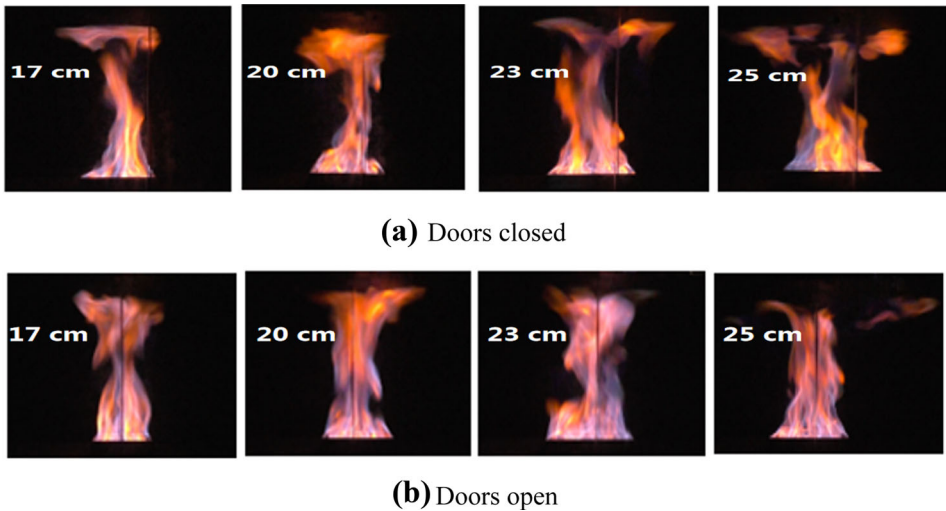
to 11.2 °C, which also shows that the effect of the door status on the longitudinal ceiling temperature is mainly on the area between the fire source and door 1. The longitudinal temperature differences raised by pan sizes of 9, 11, 13 and 15 cm are greater than 0, while those raised by large pans of 17, 20, 23 and 25 cm are less than 0. This indicates that, compared to the condition of closed doors, opening the door can accelerate the air entrainment and increase the ceiling temperature for small fires. However, when the fire is large (the critical HRR in this paper is about 11.7 kW with an equivalent full-scale HRR of 0.65 MW), the open doors act as a channel of heat losses, which oppositely reduces the temperature. Moreover, under the closed door scenario, the oxygen concentration in the compart-



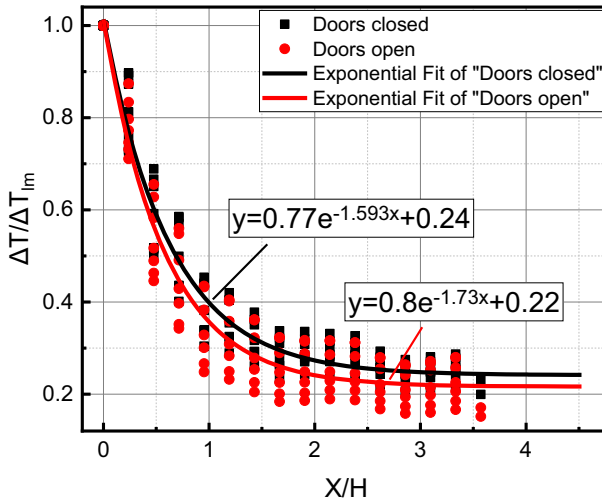
ment drops and although the flame extension is not significantly elongated in the longitudinal direction, the flame layer distributed under the ceiling thickens, as shown in Fig. 5. This also causes the ceiling temperature to rise under the closed door scenario. Hence, the above two reasons together result in the appearance that the longitudinal temperature difference shows a negative value in the case of large fires.

Figure 6 presents the dimensionless longitudinal ceiling temperature rise  $\Delta T/\Delta T_{lm}$  against the dimensionless distance from the fire source  $X/H$  for all pan sizes under different door statuses, where  $\Delta T_{lm}$  is the maximum temperature rise at the longitudinal centerline,  $X$  is the longitudinal distance from the fire source and  $H$  is the height of the subway carriage. It can be observed that both the distributions of longitudinal ceiling temperature rise under different door statuses follow an exponential decay law. The exponential decay rate for those scenarios with open doors is slightly larger than that of closed doors. This is because with open doors, the decreased temperature is due to not only the heat losses to the carriage ceiling and sidewalls but also the hot smoke exhausted from the door.

Similarly, Fig. 7 plots the transverse temperature differences between the statuses of open and closed door  $\Delta T_{l-difference}$ , at different longitudinal distances ( $X = 0, 0.5, 1.0, 1.5$  m). It can be observed that the status of the door has little effect on the transverse ceiling temperature at a distance from the fire source ( $X = 0.5, 1.0, 1.5$  m), the temperature fluctuation caused by opening the door is within  $25^\circ\text{C}$  under our experimental condition. For the transverse ceiling temperature above the fire source ( $X = 0$ ), the effect of the status of the door is significant with the increase of the fire source, especially in the scenario of the 25 cm pan (the HRR is about 24 kW, which corresponds to the full-scale fire of 1.34 MW). This result is mainly caused by two reasons. One is because of the spe-



**Figure 5. Flames from pool fires larger than 17 cm in the scenarios of doors closing and opening (front view).**



**Figure 6. Dimensionless temperature distribution at the longitudinal centerline.**

cial structure of the carriage (the lateral opening does not reach the top of the carriage in the height direction), when the heat release rate of the fire source is small, most of the fire smoke accumulates on the top of the carriage and spreads longitudinally. As the heat release rate of the fire source increases, the smoke layer sinks, part of the smoke overflows from the side doors, and the energy loss in the carriage is more obvious. At this time, the influence of the opening and closing of the door on the transverse ceiling temperature increases. The other is that when the door are open, the difference in the air entrainment on both sides of the carriage gradually becomes more significant as the fire source increases, and the flame tilts to the side with open doors, resulting in the change of the transverse temperature distribution above the fire source. This phenomenon is shown more clearly in the following ceiling smoke temperature contour profiles.

Figure 8 illustrates the dimensionless transverse ceiling temperature  $\Delta T/\Delta T_{tm,X}$  against  $Y/(W/2)$  for different longitudinal distances from the fire source ( $X = 0, 0.5, 1.0, 1.5$  m), where  $\Delta T_{tm,X}$  is the maximum transverse temperature rise at a distance of  $X$  from the fire source,  $Y$  is the transverse distance from the fire source and  $W$  is the width of the subway carriage. To systematically explore the law of transverse ceiling temperatures under different door statuses, the measured transverse temperatures between the longitudinal centerline and the sidewall without door were selected for analysis. It can be seen that the values of the dimensionless transverse ceiling temperature ( $\Delta T/\Delta T_{tm,X}$ ) far from the fire source ( $X = 0.5, 1.0, 1.5$  m) is around 1, while the dimensionless transverse ceiling temperatures ( $\Delta T/\Delta T_{tm,X}$ ) directly above the fire source ( $X = 0$ ) obey the linear attenuation law. This is because compared with the larger extension space in the longitudinal direction, the extension space in the transverse direction is confined by the sidewalls on both sides of the carriage. Therefore, in the steady-state, the transverse

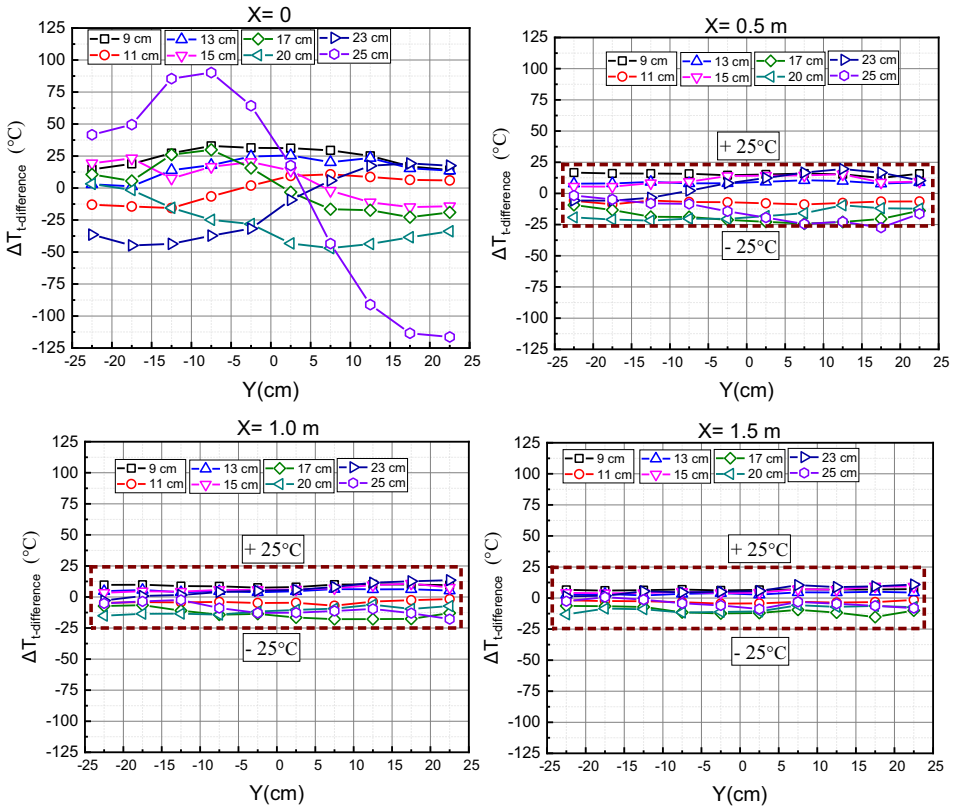
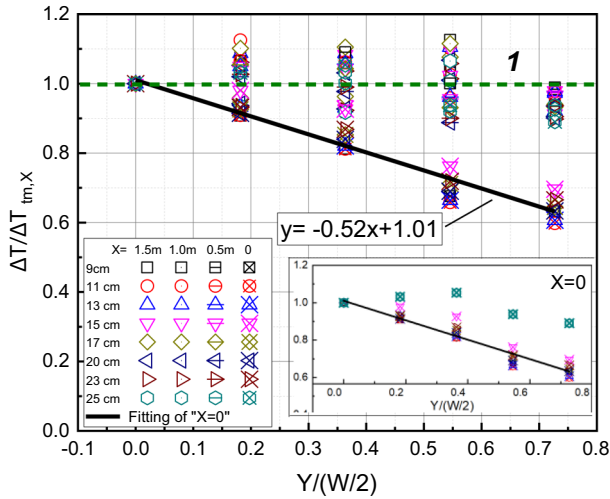


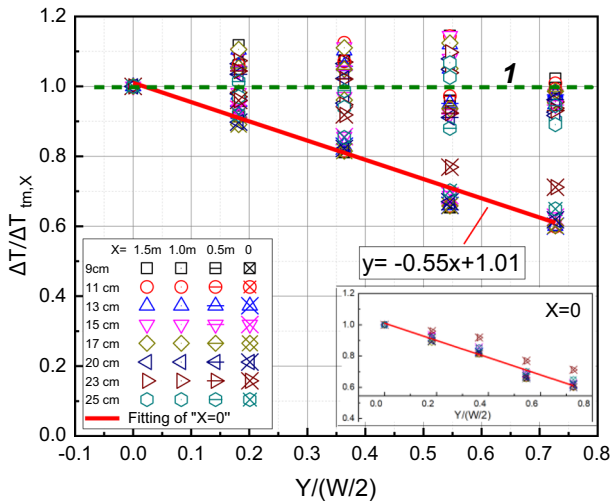
**Figure 7. The transverse temperature differences between statuses of open and closed doors at different longitudinal distances.**

ceiling temperature above the fire source does not attenuate significantly, while the transverse ceiling temperatures away from the fire source almost present isothermal phenomenon due to the continuous diffusion of the smoke stream, this phenomenon is also displayed in the following ceiling smoke temperature contour profiles. It is worth noting that, as shown in Fig. 6a, the value of the dimensionless transverse ceiling temperature directly above the fire source gradually approaches 1 instead of a regular decay in the case of a 25 cm pan. This is because with the increase of the heat release rate, the generated flame fills the entire confined space in the transverse direction, so the transverse ceiling temperature above the fire source no longer gradually decreases as the distance from the longitudinal centerline (fire source) increases for a large fire.

Figure 9 shows a typical contour profile of average temperature at a steady-state with closed doors. As the fire source is placed at the center of the carriage, it is reasonable to assume that the temperature profiles under the ceiling are axisymmetric with the transverse centerline. Taking the transverse centerline of the tunnel as the axis of symmetry (Fig. 1), the 1/2 total ceiling smoke temperature profile



(a) Doors open



(b) Doors closed

**Figure 8. Dimensionless transverse ceiling temperature distributions at different longitudinal distances.**

can be obtained based on the measurements of thermocouple arrays located 1 cm below the ceiling (Fig. 1). Through transverse symmetry, the total ceiling gas temperature profiles can be determined. It is worth noting that because the materials on both sides of the carriage are inconsistent (fire-resistant board and fire-resistant glass), there is a phenomenon that the temperature profile under the ceiling is slightly tilted toward the glass side (with the door) even when the door are closed.

However, the overall distribution of the temperature profile under the ceiling and the influence of the door on the temperature profile are the focus of this work. Therefore, the influence of this tilting phenomenon is negligible.

It can be observed that as the pan size increases, the temperature of the entire carriage ceiling gradually rises. During the steady-state, the isotherms are regularly distributed, and the isotherm values decrease as it is leaving the fire source. Also, the contour of the isotherm also gradually changes from a circular to an elliptical shape. This is because the temperature gradient decreases significantly as the longitudinal distance from the source increases, and the temperature gradient

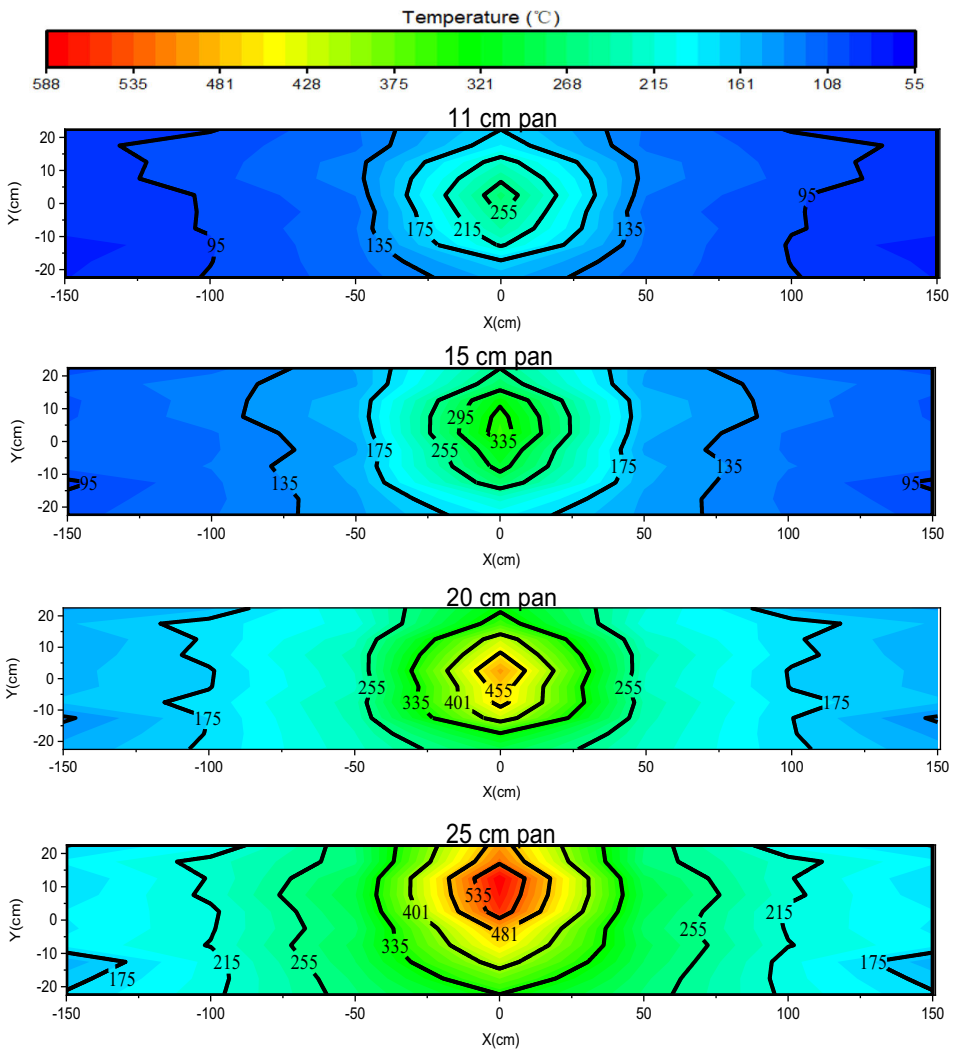


**Figure 9. Ceiling smoke temperature contour profiles for 11, 15, 20 and 25 cm pans with closed doors.**

at the same longitudinal distance gradually tends to be the same in the transverse direction, as shown in Fig. 10. This phenomenon also suggests that at the positions with the same distance away from the fire source, the temperatures along the longitudinal direction are higher than those along the transverse direction, which is consistent with Ji's research finding [26]. This is partly because of the thermal feedback when reverse smoke flow happens after the smoke hits the side walls.

Typical contour profiles of average ceiling temperature at steady-state with different doors status are shown in Fig. 11. The temperature distributions show a similar profile contour even they are under different door status for those pans less than 25 cm. It is indicated that the door status has an insignificant effect on the global temperature field under a small fire. For 25 cm pan, a noticeable difference under the two door statuses is that the high-temperature area when doors are open is slightly shifted to the sidewall with the door. The reason may be because that in the current study with small fires, the fresh air inside the carriage is sufficient to support the burning processes since both ends of the model carriage are open. Under the circumstance, the fire burning was controlled by the fuel. Therefore, the fresh air brought by the door then does not much affect the overall results, showing a limited impact on the temperature distribution. When the doors are open, as the fire increases, the strength of the air entrainment on the side with and without the door gradually becomes different, showing an asymmetrical state, so the flame is prone to incline to the sidewall, which then results in a shift high-temperature to the door.

Because the combustion state in the entire carriage is symmetrical due to the symmetrical structure of the carriage body, two doors on the left of the fire source (Door 1 and Door 2) are selected to study the temperature distributions at the door. The temperature contour profile at each door is shown in Fig. 12. It can be observed that the temperature contour profile at the door shows the regular distri-

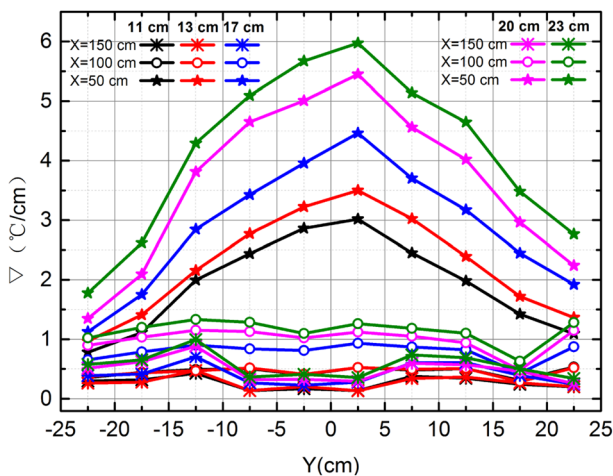


**Figure 10. Temperature gradients at different longitudinal distances from the fire source.**

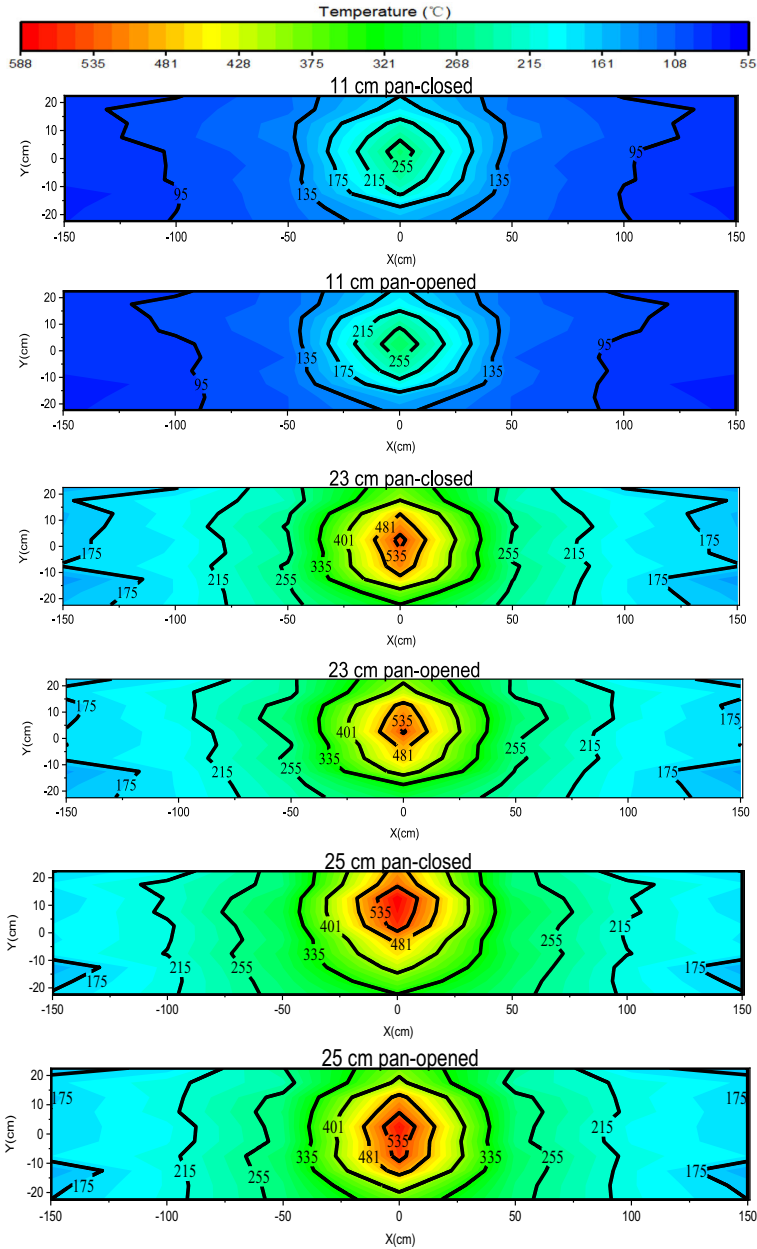


**Figure 11. Ceiling smoke temperature contour profiles for scenarios with 11, 23 and 25 cm pans.**

bution, which presents symmetrical distribution with the vertical centerline of the door as the axis of symmetry because the door is relatively small as compared with the carriage. Besides, the temperature at the door increases with the height.

In the process of growth, the isotherm gradually changes from a horizontal straight line to two inverted triangular sides. This phenomenon means that the hot smoke mainly overflows from the top of the door, the smoke concentration and temperature at the center of the door are higher than the sides during the smoke overflow process, so the middle position above the carriage door is noteworthy in the case of carriage fire.

The aforementioned analysis of the smoke temperature contour profile at the door indicates that the smoke temperature at the vertical centerline of the door is relatively high. Therefore, Fig. 13 plots the dimensionless smoke temperature rise at the vertical centerline of the door  $\frac{\Delta T}{\Delta T_{max,d}}$  against the dimensionless height from the floor  $\frac{z}{H_d}$  to obtain the attenuation trend of smoke temperature at the door with height, where  $\Delta T_{max,d}$  is the maximum temperature rise at the door,  $z$  is the height from the bottom of the door and  $H_d$  is the height of the door. It can be seen that although the temperatures of the two doors vary greatly due to the distance from the fire source, the temperatures at the two doors have the same distribution trend in the vertical height direction. Specifically, the highest temperature is at the upper part of the door but not at the highest position of the door, and the temperature at the highest position of the door is half or lower of the highest temperature at the door. Also, the dimensionless smoke temperature decays rapidly from the highest value and can be attenuated to about 0.3 after passing through the dimensionless height of 0.13. What's more, the temperature can be attenuated to ambient temperature after a dimensionless height interval of 0.26, i.e., the temperature at the door has been basically in the ambient temperature from the dimensionless height below 0.6.

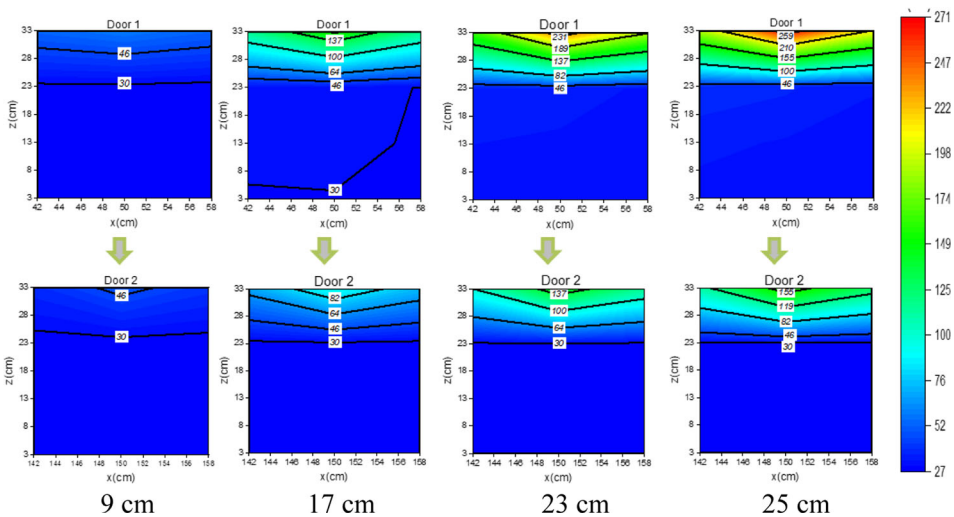


**Figure 12. Temperature contour profile at each door.**



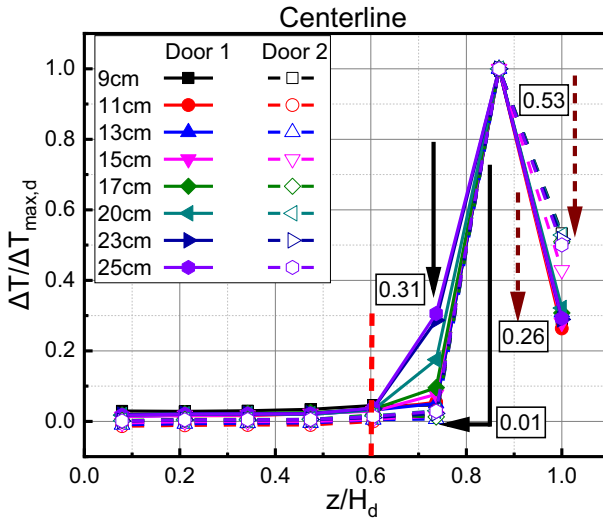


**Figure 13. Dimensionless temperature distributions at the vertical centerlines of the door.**

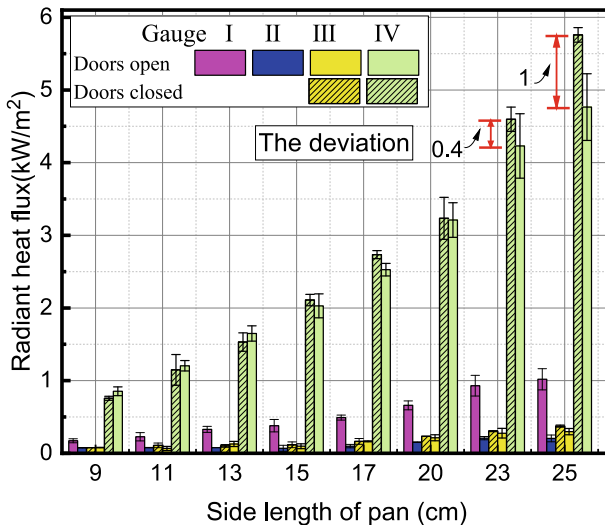
**3.3. Radiant Heat Flux**

Table 2 lists the measured average radiant heat fluxes at different spots under different scenarios. There are two measuring spots (III, IV) in the experimental scenario with the door closed, and there are four measuring spots (I, II, III, IV) in the experimental scenario with the door open. It can be seen from the table that the maximum radiant heat flux in this study can approach almost 6 kW/m<sup>2</sup>, which is related to the range of heat release rates and the type of fuel used in this study.

Figure 14 plots the histogram of radiant heat flux measurements at different spots under different opening conditions. It can be clearly seen from the figure that the radiant heat flux at the gauge I (the center of door 1) and IV (the upper part of the left end) is significantly larger than that at the gauge II (the center of door 2) and III (the center of the left end), and the radiant heat flux received at gauge IV is the largest. When the doors are closed, a similar pattern is observed, that is, the radiant heat flux at the gauge IV is much larger than that at the gauge III. The above results correspond to the characteristics that the smoke mainly flows in the upper part due to the high temperature and low density. When the doors are opened, the open doors also become one of the main passages for the smoke flow, so the center of the doors, especially the door near the fire source (gauge I in this study), also measure considerable radiant heat flux. By comparison, it can be found that the value of gauge IV (the upper part of the left end) is about 5 times that of gauge I (the center of door 1), and the ratio is not significantly affected by the pan size (heat release rate), as shown in Fig. 15. Besides the radiant heat flux received by the central position of the left end itself is relatively weak, the status of the door (open or closed) has little effect on the value of the gauge III. The measured value of the gauge IV at the upper part of

**Table 2**  
**Summary of the Measured Average Radiant Heat Fluxes at the Steady-State**

Pan size (cm)	Door status	Gauge (kW/m <sup>2</sup> )			
		I	II	III	IV
9	Closed	–	–	0.078	0.758
	Open	0.173	0.077	0.079	0.854
11	Closed	–	–	0.109	1.148
	Open	0.227	0.079	0.067	1.204
13	Closed	–	–	0.102	1.531
	Open	0.329	0.078	0.129	1.649
15	Closed	–	–	0.117	2.109
	Open	0.380	0.069	0.098	2.029
17	Closed	–	–	0.164	2.734
	Open	0.492	0.099	0.164	2.527
20	Closed	–	–	0.234	2.945
	Open	0.660	0.153	0.214	3.210
23	Closed	–	–	0.305	4.598
	Open	0.930	0.209	0.276	4.230
25	Closed	–	–	0.375	5.758
	Open	1.019	0.206	0.299	4.765



**Figure 14. Radiant heat flux at different spots under different opening conditions.**

the left end is almost unaffected by the status of the door when the pan size is small. As the pan size increases (greater than 23 cm in this paper), the measured

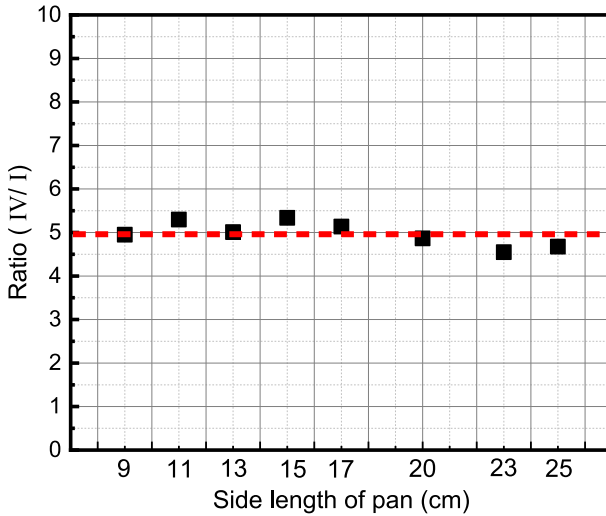


**Figure 15. The ratio of values measured by gauge IV and gauge I varies with pan size (HRR).**

value of gauge IV when the doors are closed is gradually larger than that when the doors are open, the difference between the two is gradually increased, which is because part of the hot smoke overflows from the open doors.

#### 4. Conclusions

In this paper, the reduced-scale experiments were carried out to mainly investigate the temperature contour profiles and distribution laws under the ceiling and at different doors in the subway carriage. Experimental analysis results of this study are summarized as follows:

(1) The effect of the door status on the longitudinal centerline ceiling temperature is mainly in the area between the fire source and the adjacent door. For the transverse ceiling temperature above the fire source, the effect of the door status is significant with the increase of the fire source due to the increased loss of the smoke carried through the door and the difference in the air entrainment on both sides.

(2) The temperature gradient under the ceiling decreases significantly as the longitudinal distance from the source increases, and the temperature gradient at the same longitudinal distance gradually tends to be the same in the transverse direction. The door status has an insignificant effect on the global ceiling temperature field under a small fire. As the fire increases, opening the door causes the high-temperature area to shift to the side with the door.

(3) The temperature contour profile at the door also shows regular distribution. In the process of gradually increasing the temperature as the height increases, the isotherm gradually changes from a horizontal straight line to two inverted trian-

gular sides. And the temperature at the door has been basically in the ambient temperature from the dimensionless height (normalized by the height of the door) below 0.6.

Our findings in this paper can be of use to the fire-protection community to better understand fire dynamics and provide a reference for optimizing the arrangement of the fire detection and protection systems.

## Acknowledgements

This work was supported by National Natural Science Foundation of China (No.51776192), Youth Innovation Promotion Association CAS (No. CX2320007001), Fundamental Research Funds for the Central Universities (No. WK2320000048), and the Research Grant Council of the Hong Kong Special Administrative Region, China (contract Grant Number CityU 11301015). We sincerely appreciate these supports.

## References

1. Li YZ, Ingason H (2018) Overview of research on fire safety in underground road and railway tunnels. *Tunn Undergr Space Technol* 81:568–589
2. Zhao S, Liu F, Wang F, Weng M, Zeng Z (2018) A numerical study on smoke movement in a metro tunnel with a non-axisymmetric cross-section. *Tunn Undergr Space Technol* 73:187–202
3. Zhang S, Yao Y, Zhu K, Li K, Zhang R, Lu S, Cheng X (2016) Prediction of smoke back-layering length under different longitudinal ventilations in the subway tunnel with metro train. *Tunn Undergr Space Technol* 53:13–21
4. Peng M, Shi L, He K, Yang H, Cong W, Cheng X, Richard Y (2019) Experimental study on fire plume characteristics in a subway carriage with doors. *Fire Technol* 56:1–23
5. Gao ZH, Liu ZX, Ji J, Wan HX, Sun, JH (2016) Experimental investigation on the ceiling temperature profiles of confined strong plume impinging flow. In 8th international seminar on fire and explosion hazards
6. Karlsson B, Quintiere J (1999) *Enclosure fire dynamics*. CRC Press, Boca Raton
7. Zhao S, Liu F, Wang F, Weng M (2018) Experimental studies on fire-induced temperature distribution below ceiling in a longitudinal ventilated metro tunnel. *Tunn Undergr Space Technol* 72:281–293
8. Zhang S, Cheng X, Yao Y, Zhu K, Li K, Lu S, Zhang R, Zhang H (2016) An experimental investigation on blockage effect of metro train on the smoke back-layering in subway tunnel fires. *Appl Therm Eng* 99:214–223
9. Meng N, Wang Q, Liu Z, Li X, Yang H (2017) Smoke flow temperature beneath tunnel ceiling for train fire at subway station: Reduced-scale experiments and correlations. *Appl Therm Eng* 115:995–1003
10. Delichatsios MA, Lee Y-P, Tofilo P (2009) A new correlation for gas temperature inside a burning enclosure. *Fire Saf J* 44:1003–1009

11. Tang F, Hu LH, Delichatsios MA, Lu KH, Zhu W (2012) Experimental study on flame height and temperature profile of buoyant window spill plume from an under-ventilated compartment fire. *Int J Heat Mass Transf* 55:93–101
12. Chow W (1996) Simulation of tunnel fires using a zone model. *Tunn Undergr Space Technol* 11:221–236
13. Hu LH (2006). Studies on Thermal Physics of Smoke Movement in Tunnel Fires. PH. D Thesis, University of science and Technology of China, Heifei, Anhui, China
14. Ingason H (2007) Model scale railcar fire tests. *Fire Saf J* 42:271–282
15. Li YZ, Ingason H, Lonnermark A (2014) Fire development in different scales of train carriages. *Fire Safety Science* 11:302–315
16. Lönnermark A, Ingason H, Li YZ, Kumm M (2017) Fire development in a 1/3 train carriage mock-up. *Fire Saf J* 91:432–440
17. Ng YW, Chow WK, Cheng CH, Chow CL (2019) Scale modeling study on flame colour in a ventilation-limited train car pool fire. *Tunn Undergr Space Technol* 85:375–391
18. Peng M, Cheng X, He K, Cong W, Shi L, Yuen R (2020) Experimental study on ceiling smoke temperature distributions in near field of pool fires in the subway train. *J Wind Eng Ind Aerodyn* 199:104135
19. Carvel R, Beard A (2005) *The Handbook of Tunnel Fire Safety*. Thomas Telford, London
20. Yao Y, Cheng X, Shi L, Zhang S, He K, Peng M, Zhang H (2018) Experimental study on the effects of initial sealing time on fire behaviors in channel fires. *Int J Therm Sci* 125:273–282
21. Shafee S, Yozgatligil A (2018) An analysis of tunnel fire characteristics under the effects of vehicular blockage and tunnel inclination. *Tunn Undergr Space Technol* 79:274–285
22. Fan CG, Ji J, Li YZ, Ingason H, Sun JH (2017) Experimental study of sidewall effect on flame characteristics of heptane pool fires with different aspect ratios and orientations in a channel. *Proc Combust Inst* 36:3121–3129
23. Chen C-k, Zhu C-x, Liu X-y, Kang H, Zeng J-w, Yang J (2016) The effect of fuel area size on behavior of fires in a reduced-scale single-track railway tunnel. *Tunn Undergr Space Technol* 16(52):127–137
24. Chen C-k, Xiao H, Wang N-n, Shi C-l, Zhu C-x, Liu X-y (2017) Experimental investigation of pool fire behavior to different tunnel-end ventilation opening areas by sealing. *Tunn Undergr Space Technol* 63:106–117
25. Chen C-k, Zhu C-x, Liu X-y, Yu N-h (2016) Experimental investigation on the effect of asymmetrical sealing on tunnel fire behavior. *Int J Heat Mass Transf* 92:55–65
26. Ji J, Fu YY, Fan CG, Gao ZH, Li KY (2015) An experimental investigation on thermal characteristics of sidewall fires in corridor-like structures with varying width. *Int J Heat Mass Transf* 84:562–570
27. Ji J, Bi Y, Venkatasubbaiah K, Li K (2016) Influence of aspect ratio of tunnel on smoke temperature distribution under ceiling in near field of fire source. *Appl Therm Eng* 106:1094–1102